Analysis of Some Modified Cell-Averaging CFAR Processors in Multiple-Target Situations

M. WEISS
RAFAEL—Armament Development Authority, Israel

A serious degradation of detection probability (P_d) in a cell-averaging constant false alarm rate (CA-CFAR) detector is known to be caused by the presence of an interfering target in the set of reference cells.

A technique which is often used to prevent excessive false alarms at clutter "edges" is a "greatest of" (GO) selection between the leading and lagging sets of cells (GO-CFAR). However, it is demonstrated for a Rayleigh target that the abovementioned suppression effect is more acute in the GO-CFAR. Practically, detection of closely separated targets is almost inhibited.

Selection of the "smallest of" (SO) the means for the adaptive threshold has been proposed to alleviate this problem. An analytic expression for P_d of this detector is also derived, and it is shown that though it does prevent the suppression effect, a large sensitivity loss is introduced unless the number of reference cells is sufficiently large. A modified CO-CFAR detector, combining a "censoring" circuit, is proposed for automatic detection in a complex nonhomogeneous environment.

Manuscript received January 13, 1981; revised March 22, and June 8, 1981.

Author's address: RAFAEL—Armament Development Authority, P.O. Box 2250, Haifa, Israel 31021 (88).

0018-9251/82/0100-0102 $00.75

I. INTRODUCTION

Automatic detection of radar targets in a nonstationary noise and clutter background is commonly implemented by comparing the processed voltage from each resolution cell to an adaptive threshold, obtained from estimates of the mean level of the interference over adjacent range and/or Doppler cells [1]. When the interference is homogeneous over the reference cells, constant false alarm rate is achieved. In the cell-averaging constant false alarm rate (CA-CFAR) detector the threshold is obtained from the arithmetic mean of the video outputs of a number M of adjacent cells. When the interference is also Gaussian distributed, the CA-CFAR maximizes the detection probability P_d [2, 3], and as M increases P_d approaches that of the classical Neyman-Pearson case, where the mean level of interference is known a priori. Performance of the CA-CFAR with different detector laws (square law, envelope, logarithmic), postdetection integration modes (video or binary) and various target models has been described and analyzed in the literature [1-8].

Most CFAR processors (including other parametric and distribution-free detectors) cannot maintain the optimal performance when certain, generally held assumptions about the environment are violated. For the CA-CFAR, the inherent assumption is that the statistics of the interference at each reference cell are the same as the statistics of the test cell. There are two common situations in which this condition is not met.

1) *Edges*: One common situation is step increases in the background noise level, such as that produced at clutter or chaff edges. This situation was analyzed in [1, 9, 10] and other papers and causes two different effects:

a) If the cell under test is in the clear region but a group of the reference cells are immersed in the clutter edge, a masking effect results. The threshold is raised unnecessarily and therefore P_d (along with P_{fa}) is lowered significantly, even though there is a high signal-to-noise ratio (SNR) in the cell of interest. Thus with the CA-CFAR the clutter regions are actually expanded at each edge by about a half-length of the reference window ($M/2$).

b) On the other hand, if the test cell is immersed in the clutter return but some of the reference cells are in the clear, then P_{fa} increases intolerably with an increase in the interference level discontinuity. (A 20 dB discontinuity amounts to 3 to 4 orders of magnitude in P_{fa} [1, 9].)

The last problem is of primary concern in a search radar design. Hansen [9] proposed a modification to the CA approach, which can control the false alarms at the edges. It is known as the greatest-of detector (GO-CFAR). As shown in [9] and in Moore and Lawrence [10], P_{fa} remains almost constant as the reference window sweeps over the edge. (However, the masking effect discussed above is obviously worsened.) The additional detectability loss introduced by the GO-CFAR (when the background noise is homogeneous) was determined in [10] and by Hansen and Sawyers [11] and is quite small; typically it falls in the range of 0.1 to 0.3 dB.

2) *Target returns in the reference window*: When another target (denoted hereafter as the interfering target) lies within the reference cells of the target in question (denoted hereafter as the primary target), the threshold is raised and detection of the primary target is seriously degraded. Closely separated targets are probable in either a civil or a military dense target environment, e.g., for a radar with compressed pulsewidth of 1 μs and CA-CFAR with 16 cells on each side of the test cell, if two targets are within one antenna beamwidth and are separated in range less than 2.4 km, the described suppression occurs. Finn and Johnson [1] and Rickard and Dillard [12] analyzed this problem and demonstrated that, for all of the single-pulse Swerling target fluctuation models (i.e., cases 0, 1, and 3), the probability of detecting the primary target is asymptotic to values significantly less than unity, as the SNR of the two target returns approaches infinity while the cross sections are proportional. Similar behavior is encountered in a distribution-free detector [13].

It is obvious that the above "capture" phenomena is more acute in the GO-CFAR. This is shown analytically for Swerling I targets in the first part of the paper.

Trunk [14] has considered the target range-resolution properties of some adaptive threshold detectors. He has shown that even if the targets are large enough to be detected, they would not be resolved by a CA-CFAR detector provided one is within the reference cells of the other. To improve resolution, it was then recommended that the CA-CFAR should be modified such that the threshold is obtained from the smallest-of (SO) the means of either the leading or the lagging part of the reference window. However, Trunk's simulation of the SO-CFAR was for a high SNR (20 dB) and a large number of reference cells ($M = 20$). It is shown in the second part of the paper that the SO-CFAR modification is less sensitive than the basic CA-CFAR, in a homogeneous background, unless M is large enough (e.g., for $P_{fa} = 10^{-6}$ Swerling I targets, the additional detectability loss is about 11 dB when $M = 4$ but only 0.7 dB when $M = 32$). An analytic expression for P_d of a Swerling I target, when one interfering target with infinite SNR lies within the reference window, is also derived. It is shown that even in this severest situation the additional SNR loss of the SO-CFAR (relative to the case without an interfering target) is minimal, and P_d is asymptotic to unity with increase of SNR, i.e., the capture effect encountered in both the CA and GO-CFAR is avoided using the SO-CFAR.

In the last part of this paper the tradeoffs concerning selection of the appropriate type of detector and an adequate choice of M are discussed. A modified CA-CFAR detector, which combines a GO selection together with censoring circuits which discard the highest cell output from the leading and lagging windows, is proposed as a solution to the automatic detection problem in a complex nonhomogeneous environment consisting of both clutter edges and closely separated targets.

II. THRESHOLD STATISTICS OF THE MODIFIED CA-CFAR DETECTORS

The various modifications of the basic CA-CFAR detector considered in this paper are shown in Fig. 1. Two reference windows (U, V) are formed from the sum of $M/2$ cell outputs on the leading and lagging side of the test cell. (The samples are taken from either range or Doppler domains, or from some combination of both.) The output of the selection logic (Q) is the sum of the two window outputs in the basic CA-CFAR, and the greatest or smallest of the outputs in the GO-CFAR and SO-CFAR modifications, respectively.

The analysis will be carried for the case where the background is white Gaussian noise, and the M reference range samples that are used to estimate the ambient interference power are statistically independent. It is assumed that the $M + 1$ taps contain two target signals; one at the center tap (for which a detection decision is to be made), and the other (regarded as extraneous or interfering) at some arbitrary cell of the M. The role of the targets is interchanged when the radar range is swept, i.e., the nearest target is initially the primary one and afterwards the interfering, and vice versa.[1] Both targets fluctuate with Rayleigh amplitude distribution. (This model is a common one and enables simple, closed-form calculations.) The signal processing in Fig. 1 does not include any noncoherent integration; the input to the square-law detector corresponds either to a radar with single-pulse detection, or to the output of one of the narrowband Doppler filters of a pulse-Doppler radar. In the last case, the following analysis holds for slowly fluctuating targets (Swerling case I), and the single-pulse SNR should be replaced with the coherently integrated SNR at the output of the Doppler filter.

[1]The problem considered is that of detecting either target individually. Our results can be easily modified for a case of detecting at least one of the two targets.

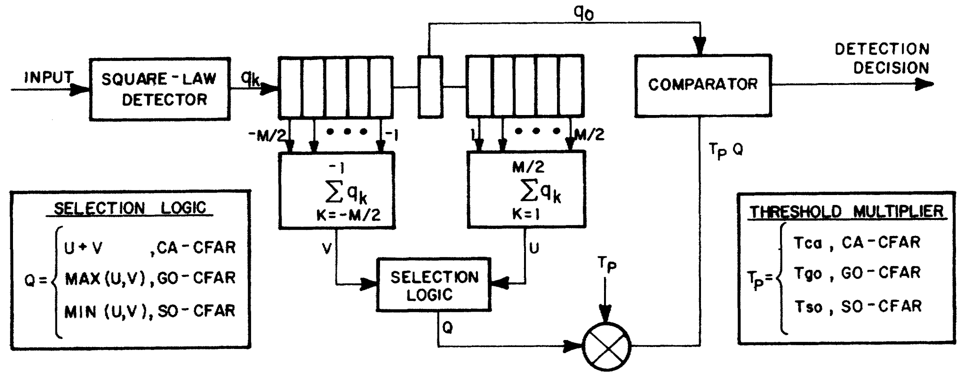

Fig. 1. Modified CA-CFAR processor.

Since both the noise and Rayleigh targets have Gaussian quadrature components, the output of the square-law detector q_K $(K = -M/2, \ldots, M/2)$ has an exponential probability density function (pdf). For the detection cell,

$$ {}_hP_q(q_0) = (1/2\sigma_h^2)\exp(-q_0/2\sigma_h^2), \qquad q_0 \geqslant 0, \quad h = 0, 1 \tag{1}$$

where $h = 0, 1$ indicates the noise only or signal plus noise hypothesis, respectively, and σ_h^2 is defined as

$$\sigma_h^2 = \begin{cases} \sigma^2, & h = 0 \\ \sigma^2(1 + S), & h = 1 \end{cases} \tag{2}$$

where σ^2 is the unknown, average noise power at the detector input, and S is the SNR of the primary target. The pdf of the reference cells containing noise only is identical to ${}_0P_q(q_K)$, and the pdf of the arbitrary cell containing the interfering target is identical to ${}_1P_q(q_K)$ given in (1), but S is replaced with I, defined as the SNR of the interfering target.

The detection probability in the presence of the interfering target for detector $p(p$ = CA, GO, SO), denoted as $P_d^p(s, I)$, is obtained by integrating the detection probability, conditional on a fixed value of the threshold T_pQ, over the pdf of the background noise estimator $P_Q^p(Q)$:

$$P_d^p(S, I) = \int_0^\infty \Pr(q_0 > T_pQ|Q, H_1)P_Q^p(Q)\,dQ \tag{3}$$

where

$$\Pr(q_0 > T_pQ|Q, H_1) = \int_{T_pQ}^\infty {}_1P_q(q_0)\,dq_0 = \exp[-T_pQ/2\sigma^2(1 + S)]. \tag{4}$$

The cumulative distribution function (CDF) of Q with the modified processors is given by [15]

$$F_Q^{GO}(Q) = F_u(Q)\,F_v(Q) \tag{5}$$

for the GO-CFAR, and by

$$F_Q^{SO}(Q) = F_u(Q) + F_v(Q) - F_u(Q)\,F_v(Q) \tag{6}$$

for the SO-CFAR. The pdf's are found by differentiation, which yields

$$P_Q^{GO}(Q) = (d/dQ)\,F_Q^{GO}(Q) = P_u(Q)\,F_v(Q) + F_u(Q)\,P_v(Q) \tag{7}$$

$$P_Q^{SO}(Q) = (d/dQ)\,F_Q^{SO}(Q) = P_u(Q)\,[1 - F_v(Q)] + P_v(Q)\,[1 - F_u(Q)]. \tag{8}$$

In contrast to the stationary situation analyzed in [10] and [11], U and V are no longer identically distributed due to the interfering target. Assuming that the extraneous target is in one of the leading cells (V), U is χ^2 distributed with $2(M/2)$ degrees of freedom; thus

$$P_u(U) = U^{M/2-1}\exp(-U)/(M/2 - 1)!, \qquad U \geqslant 0. \tag{9}$$

(For convenience, U, V, and q_0 are all normalized by division with $2\sigma^2$), and by integrating (9),

$$F_u(U) = 1 - \exp(-U)\sum_{K=0}^{M/2-1} U^K/K!, \qquad U \geqslant 0. \tag{10}$$

It is shown in Appendix A that for V,

$$P_v(V) = (1/I)[(1 + I)/I]^{M/2-2}\{\exp[-V/(1 + I)] - \exp(-V)\sum_{k=0}^{M/2-2}(1/k!) \cdot [VI/(1 + I)]^k\} \tag{11}$$

and

$$F_v(V) = 1 - [(1 + I)/I]^{M/2-1}$$
$$\cdot \exp[-V/(1 + I)] + (1/I)\exp(-V)$$
$$\cdot \sum_{k=0}^{M/2-2} [(1 + I)/I]^k$$
$$\cdot \sum_{l=0}^{M/2-2-k} (V^l/l!). \quad (12)$$

With the substitution of (9) through (12) into (7) and (8), the threshold pdf's are obtained. Then $P_d^p(S, I)$ can be expressed in a closed form by substitution of (7) or (8) and (4) into (3) and performing the integration.

III. CELL-AVERAGING CFAR WITH GREATEST OF SELECTION LOGIC

The basic CA-CFAR processors assume that the reference observations are representative of the noise in the detection cell. Clutter residues and jamming can, however, exhibit a significant power level variation as a function of range (or Doppler, when the noise estimate is derived from different Doppler filters), and precautions must be taken to avoid false alarms due to clutter edges, for example. A technique [9] which is often used to prevent these excessive false alarms, is to estimate the background noise level independently from the leading and lagging reference cells and to use the greatest of these two estimates as the adaptive threshold, as shown in Fig. 1.

The additional detectability loss introduced by this modification (when the background noise is stationary) was determined in [11] and is quite small; typically it falls in the range of 0.1 to 0.3 dB. However, when an interfering target lies in the reference cells, performance degradation is even worse than with the basic CA-CFAR processor. This can be grasped intuitively, since when I is large enough, the half-portion of the delay line containing the extraneous target is almost always selected; hence the threshold is raised higher and detectability loss is further increased.

The above argument can be proven analytically for the same noise and targets statistics as has been assumed before. Since the integration of (3) results in a very cumbersome expression for $P_d^{GO}(S, I)$, it will be tracked here only in the limit when the SNR of both targets approaches infinity, in such a way that the ratio I/S remains constant (i.e., the target cross sections are proportional). Then, it is shown in Appendix B that

$$\lim_{\substack{I, S \to \infty \\ I/S = \text{constant}}} P_d^{GO}(S, I) = [1 + (I/S)\, T_{GO}(P_{fa}, M)]^{-1} \quad (13)$$

TABLE I
Threshold Multipliers T_{GO} of the GO CA-CFAR versus P_{fa} and M (Total Number of Reference Cells)

	M			
P_{fa}	4	8	16	32
10^{-4}	14.0	3.60	1.36	0.602
10^{-5}	26.2	5.39	1.85	0.785
10^{-6}	47.8	7.78	2.42	0.983
10^{-7}	86.5	11.0	3.08	1.196
10^{-8}	155.1	15.3	3.84	1.425

where $T_{GO}(P_{fa}, M)$ is the threshold multiplier in a GO-CFAR with total of M reference cells, which is needed to achieve the *design* P_{fa} (i.e., when the interfering target is absent). It is clearly seen that increasing the primary target SNR (S) to infinity does not cause the detection probability to approach 1.0, when the two target returns have proportional cross sections. The corresponding result for the CA-CFAR with Swerling I targets is [12]

$$\lim_{\substack{S, I \to \infty \\ I/S = \text{constant}}} P_d^{CA}(S, I) = [1 + (I/S)\, T_{CA}(P_{fa}, M)]^{-1} \quad (14)$$

Although (13) and (14) are of the same form, it is not implied that $P_d^{GO} = P_d^{CA}$ for equal I/S. The threshold multiplier T_{GO} is always higher than T_{CA} of the basic CA-CFAR and is found by an iterative solution of [11, eq. (7)]

$$P_{fa}/2 = (1 + T)^{-M/2} - (2 + T)^{-M/2} \cdot \sum_{k=c}^{M/2-1} \binom{M/2 - 1 + k}{k} (2 + T)^{-k} \quad (15)$$

for the setting $T = T_{GO}(P_{fa}, M)$ which results in the specified P_{fa}. The appropriate T_{GO} values for $M = 4$, 8, 16, 32, and $P_{fa} = 10^{-4}, 10^{-5}, 10^{-6}, 10^{-7}, 10^{-8}$ are summarized in Table I. The corresponding threshold multipliers for the basic CA-CFAR are given by $T_{CA}(P_{fa}, M) = P_{fa}^{-1/M} - 1$, and are smaller for any (P_{fa}, M), as has been claimed above.

For demonstration of the higher degradation of the GO-CFAR in a multiple target situation, let us define the additional CFAR loss ΔL_{GO}, due to the greatest of selection in the presence of one interfering target (relative to the CA-CFAR), as the required (dB) increase in S/I (or in the target cross sections ratio), for the same specified P_{fa} and $P_d(I, S)$ in both processors, when both S and $I \to \infty$. From (13) and (14),

$$\Delta L_{GO} \triangleq 10\log[(S/I)_{GO}/(S/I)_{CA}]$$
$$= 10\log[T_{GO}(P_{fa}, M)/(P_{fa}^{-1/M} - 1)]. \quad (16)$$

TABLE II
Additional CFAR Loss ΔL_{GO} in dB for the GO Processor With One Interfering Target

M	4	8	16	32
ΔL_{GO} (dB)	1.94	2.26	2.47	2.60

Note: $P_{fa} = 10^{-6}$, I and $S \to \infty$.

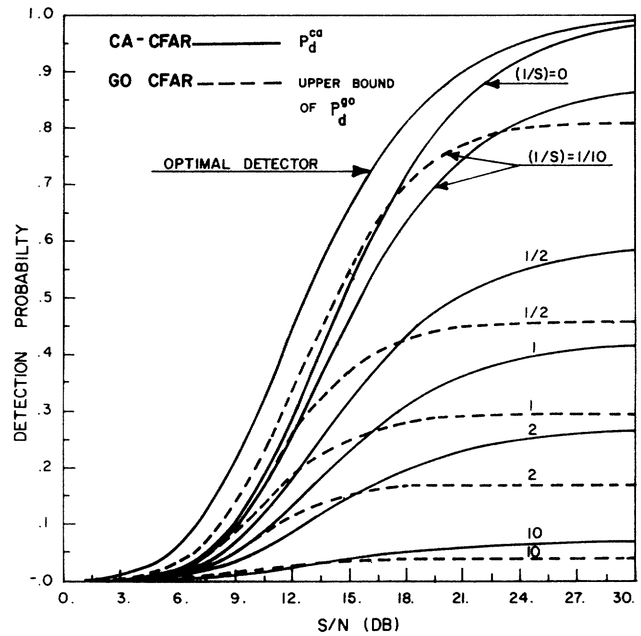

Fig. 2. Detection probability of the CA and GO-CFAR processors versus primary target SNR (one interfering target, $P_{fa} = 10^{-6}$, $M = 16$, $I/S = 0, 1/10, 1/2, 1, 2, 10$).

TABLE III
Probability of Detection for Basic and GO-CFAR Processors versus P_{fa} and M

	M							
	CA-CFAR, $P_d^{CA}(\infty, \infty)$				GO-CFAR, $P_d^{GO}(\infty, \infty)$			
P_{fa}	4	8	16	32	4	8	16	32
10^{-4}	0.100	0.316	0.562	0.750	0.067	0.217	0.424	0.624
10^{-5}	0.056	0.237	0.488	0.698	0.037	0.156	0.351	0.560
10^{-6}	0.032	0.178	0.422	0.650	0.020	0.114	0.292	0.504
10^{-7}	0.018	0.134	0.365	0.604	0.011	0.083	0.245	0.455
10^{-8}	0.010	0.100	0.316	0.562	0.006	0.061	0.207	0.412

Note: Both targets have an equal and infinite SNR ($I = S$, I and $S \to \infty$).

Table II shows ΔL_{GO} for $P_{fa} = 10^{-6}$. The (dB) values for the other P_{fa} in the range 10^{-4} to 10^{-8} are within ± 2 percent of those shown.

An alternative demonstration of the emphasized capture effect in this processor is shown in Table III, which compares the achieved detection probability in the two processors, when both targets have an equal and infinite SNR ($I/S = 1$).

Fig. 2 shows the detection probability for the CA and GO-CFAR detectors as a function of the primary target SNR (S), for $P_{fa} = 10^{-6}$, $M = 16$, and different values of I/S. The solid curves are for the CA-CFAR; they were calculated from [12, fig. 7]:

$$P_d^{CA}(S, I) = \{[1 + (P_{fa}^{-1/M} - 1)/(1 + S)]^{M-1} \cdot [1 + (1 + I)(P_{fa}^{-1/M} - 1)/(1 + S)]\}^{-1}. \quad (17)$$

The dashed curves are an upper limit of $P_d^{GO}(I, S)$ and were calculated from (B4) of Appendix B. Also shown is the curve for the optimal detector with the noise power known a priori ($P_d = P_{fa}^{1/(1+S)}$). Although the results in Fig. 2 are for a Swerling I target model, it is believed that a similar capture effect is to be expected for other target models (i.e., nonfluctuating and Swerling III).

IV. CELL-AVERAGING CFAR WITH SMALLEST OF SELECTION LOGIC

The SO-CFAR detector has been recommended by Trunk [14] in order to improve resolution of closely spaced targets. In this detector the adaptive threshold is obtained from the smallest of the means of either the leading or the lagging part of the reference window, as shown in Fig. 1. It is obvious that this procedure will cause an excessive number of false alarms unless the clutter is cancelled to the thermal noise level, by some form of multiple target indicator (MTI) or potential difference (PD) processing.[2]

[2]If the cancellation is not sufficient a residual clutter edge remains, and when the test cell is in its higher side, the threshold which is generated from the lower side is too low and causes a false alarm.

When considering resolution algorithms for an automatic detector, one should consider also its sensitivity, i.e., the detection loss which it introduces in homogeneous background. However, this was not treated in [14] and will be evaluated in the following along with the SO-CFAR performance in a multiple target environment.

Since, in a stationary background with no interfering target, U and V are identically distributed, from (8)

$$P_Q^{SO}(Q) = 2P_u(Q)[1 - F_u(Q)]. \tag{18}$$

Upon substituting (9) and (10) into (18) and then into (3) and performing the integration, we obtain

$$P_d^{SO}(S, I = 0) = \{2/[2 + T_{SO}/(1 + S)]^{M/2}\} \cdot \sum_{k=0}^{M/2-1} \binom{M/2 - 1 + k}{k} \{1/[2 + T_{SO}/(1 + S)]^k\}. \tag{19}$$

For $S = 0$ this expression also yields P_{fa}. A numerical solution is needed to solve (19) for the threshold multiplier T_{SO} (P_{fa}, M). The results for $M = 4, 8, 16, 32$, and $P_{fa} = 10^{-4}, 10^{-5}, 10^{-6}$ are summarized in Table IV.

The detection probability without an interfering target is shown in Figs. 3 through 5 for $P_{fa} = 10^{-4}$, 10^{-6}, and 10^{-8}, respectively, and for $M = 4, 8, 16$, and 32. In each figure the solid curves are P_d^{SO} (S, $I = 0$) from (19), and the dashed curves correspond to P_d^{CA} (S, $I = 0$); i.e., the detection probability of the basic CA-CFAR in a homogeneous background, which is obtained upon substituting $I = 0$ into (17). The additional CFAR loss ΔL_{SO} (I), relative to the basic CA-CFAR without an interfering target, is defined here[3] as the required SNR (dB) increase, for the same specified P_{fa} and P_d in both processors,

$$\Delta L_{SO}(I) = 10 \log[S_{SO}(P_{fa}, P_d, I)/S_{CA}(P_{fa}, P_d)]. \tag{20}$$

It is clearly seen that $\Delta L_{SO}(0)$ is quite large for a small number of test cells[4], and that as M increases, the loss asymptotically vanishes. Also, the loss is almost independent of P_d (dB changes of few percents for P_d from 0.05 to 0.95) and is higher for smaller P_{fa}, as expected. The losses for $P_d = 0.5$ and the above values of M and P_{fa} are given in Table V. It can be concluded that the SO-CFAR should not be used unless M is large enough.

[3]The definition (20) is not equivalent to (16); for the GO-CFAR the additional loss in S/I was considered.

[4]We reemphasize that δL_{SO} is an additional loss relative to the CA-CFAR, which also introduces a large loss relative to the optimal Neyman-Pearson detector when M is small, e.g., the loss of the basic CA-CFAR is 9.3 dB for $M = 4$, $P_{fa} = 10^{-6}$, and $P_d = 0.5$.

TABLE IV
Threshold Multipliers T_{SO} of the SO-CFAR versus P_{fa} and M

	M			
P_{fa}	4	8	16	32
10^{-4}	140.1	10.88	2.444	0.8515
10^{-6}	1410	36.58	5.131	1.475
10^{-8}	14140	117.9	9.905	2.302

TABLE V
SO-CFAR Additional Loss ΔL_{SO} (0), (dB), versus M and P_{fa}, Without an Interfering Target ($P_d = 0.5$)

	M			
P_{fa}	4	8	16	32
10^{-4}	6.63	2.58	0.99	0.41
10^{-6}	16.3	4.51	1.76	0.70
10^{-8}	16.2	6.69	2.64	1.05

The detection probability with an interfering target of arbitrary SNR (I) was obtained in closed form by the equations of Section II. Since the resulting expression is very cumbersome, we give the result only for the severest case of infinite I. Substituting (B1) and (B2) from Appendix B along with (9) and (10) into (8) and then into (3), we obtain

$$P_d^{SO}(S, I \to \infty) = \{(1 + S)I/[IT_{SO} + (1 + S)(1 + I)]\}^{M/2} + (1/I) \cdot \sum_{k=0}^{M/2-1} \{(1 + S)I/[IT_{SO} + (1 + S)(1 + I)]\}^{k+1}. \tag{21}$$

Thus a lower bound for P_d^{SO} is

$$\lim_{I \to \infty} P_d^{SO}(S, I) = [1 + T_{SO}(P_{fa}, M)/(1 + S)]^{-M/2}. \tag{22}$$

Equation (22) is plotted versus S in Figs. 6 through 9 for $M = 4, 8, 16$, and 32 and for $P_{fa} = 10^{-6}$. Also shown in these figures is the detection probability of the SO-CFAR without an interfering target, $P_d^{SO}(S, 0)$, and of the CA-CFAR with an interfering target with $I/S = 1$, $P_d^{CA}(S, I = S)$, and without it, $P_d^{CA}(S, I = 0)$.

The asymptotic values for the GO-CFAR, $P_d^{GO}(S \to \infty, I = S)$ given in (13) are also indicated on the right-hand margins of the figures. It is clearly seen that the serious suppression of detection that is caused by the presence of the interfering target in one of the reference cells of either the CA or the GO-CFAR, is almost eliminated by the SO-CFAR (i.e., when the primary target SNR is increased, P_d is asymptotic to unity). It is also seen from the above figures that, again, the loss $\Delta L_{SO}(I \to \infty)$ is almost independent of

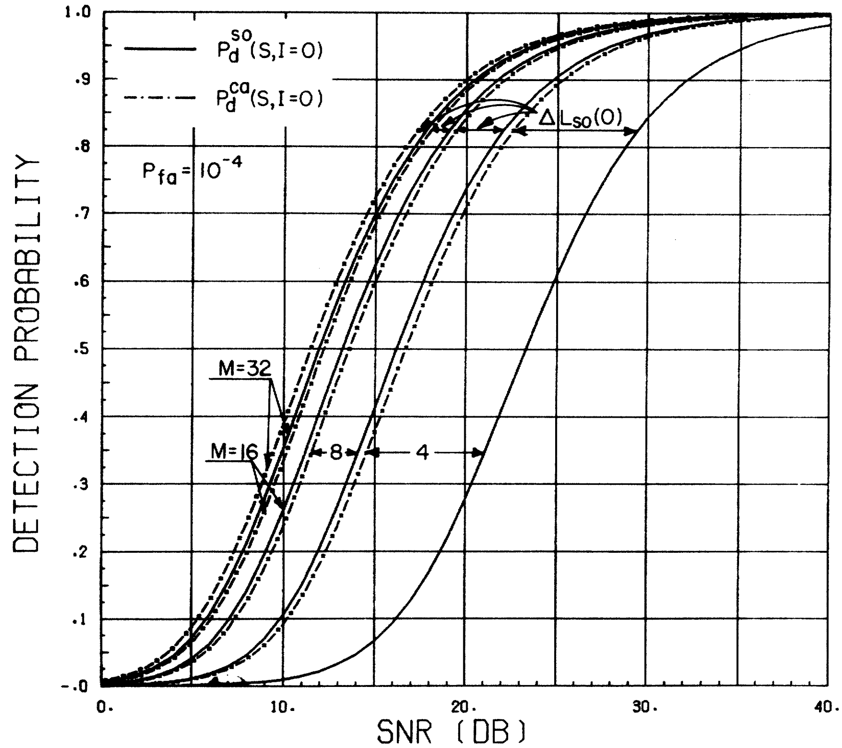

Fig. 3. Detection probability of the CA and SO-CFAR processors versus SNR, without interfering target (M = 4, 8, 16, 32; P_{fa} = 10^{-4}).

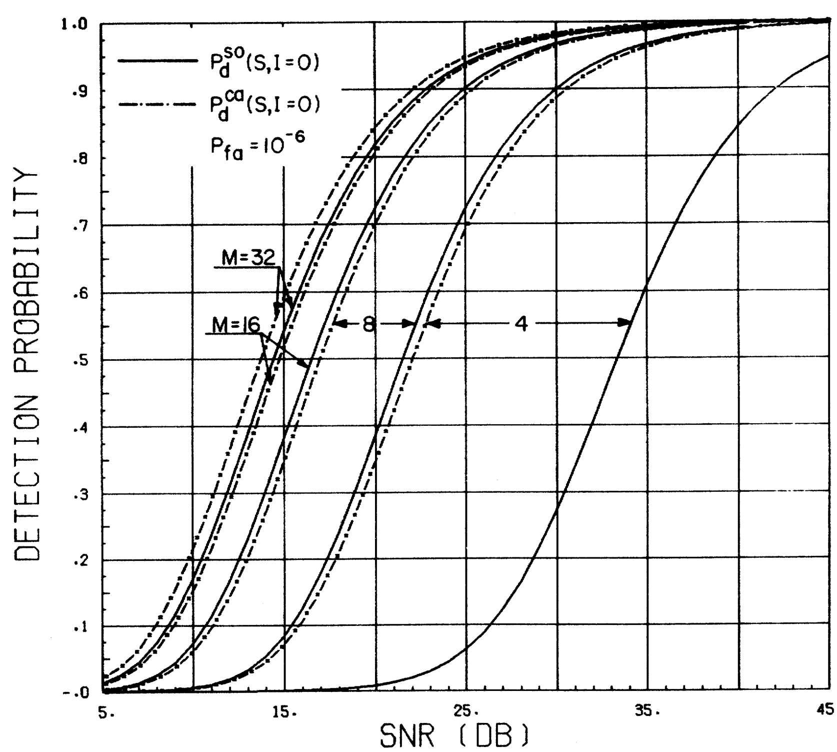

Fig. 4. Detection probability of the CA and SO-CFAR processors versus SNR, without interfering target (M = 4, 8, 16, 32; P_{fa} = 10^{-6}).

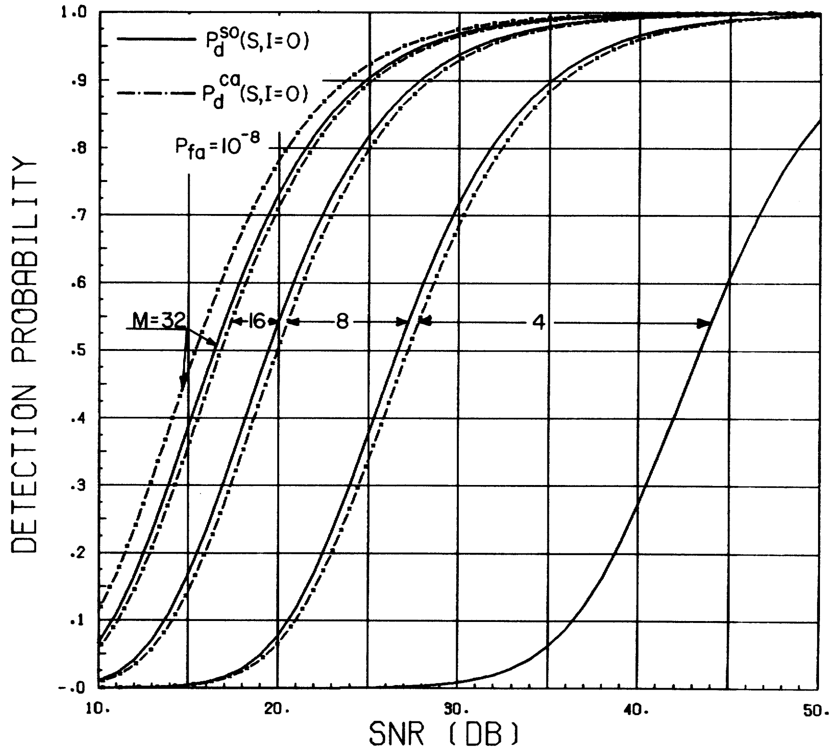

Fig. 5. Detection probability of the CA and SO-CFAR processors versus SNR, without interfering target (M = 4, 8, 16, 32; P_{fa} = 10^{-8}).

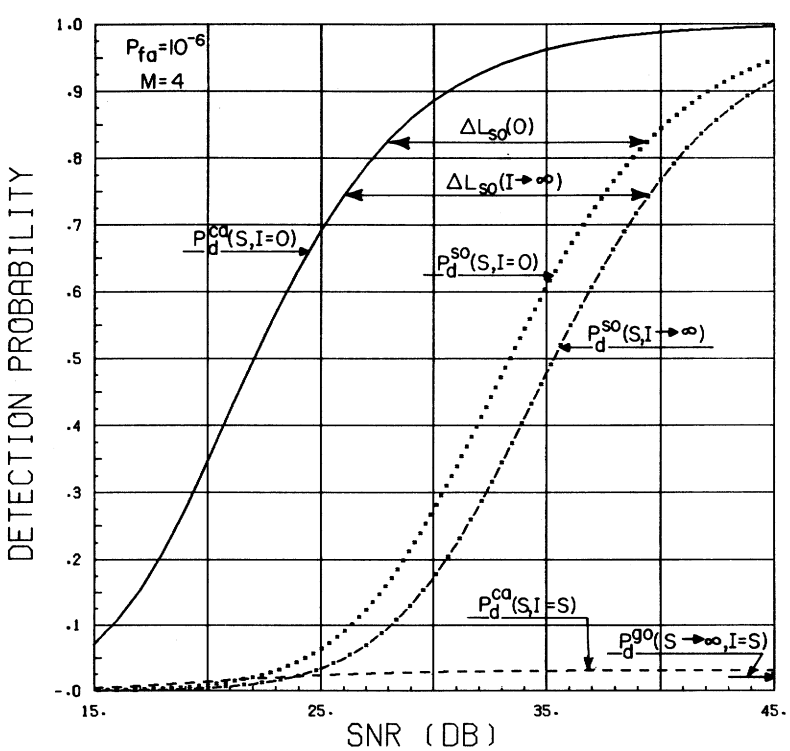

Fig. 6. Detection probability versus primary target SNR. P_d^{SO} (S, I = 0): SO-CFAR without interfering target. P_d^{SO}(S, $I \to \infty$): SO-CFAR with infinite SNR interfering target. P_d^{CA} (S, I = 0): CA-CFAR without interfering target. P_d^{CA} (S, I = S): CA-CFAR with interfering target whose SNR is equal to primary's. P_d^{GO} ($S \to \infty$, I = S): GO-CFAR when both targets have equal and infinite SNR (P_{fa} = 10^{-6}, M = 4).

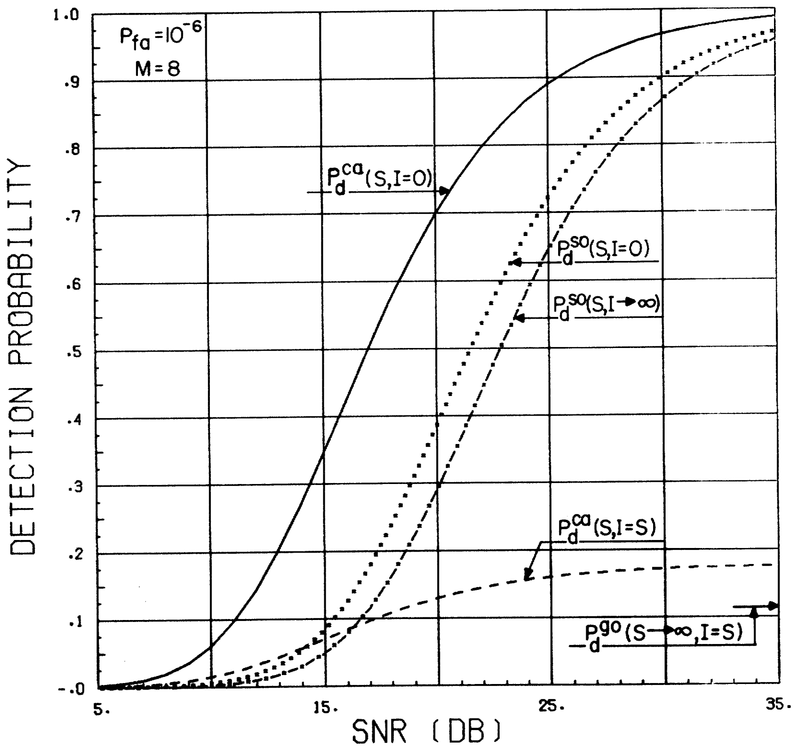

Fig. 7. Detection probability versus primary target SNR. P_d^{SO} $(S, I = 0)$: SO-CFAR without interfering target. P_d^{SO} $(S, I \rightarrow \infty)$: SO-CFAR with infinite SNR interfering target. P_d^{CA} $(S, I = 0)$: CA-CFAR without interfering target. P_d^{CA} $(S, I = S)$: CA-CFAR with interfering target whose SNR equal to primary's. $P_d^{GO}(S \rightarrow \infty, I = S)$: GO-CFAR when both targets have equal and infinite SNR ($P_{fa} = 10^{-6}$, $M = 8$).

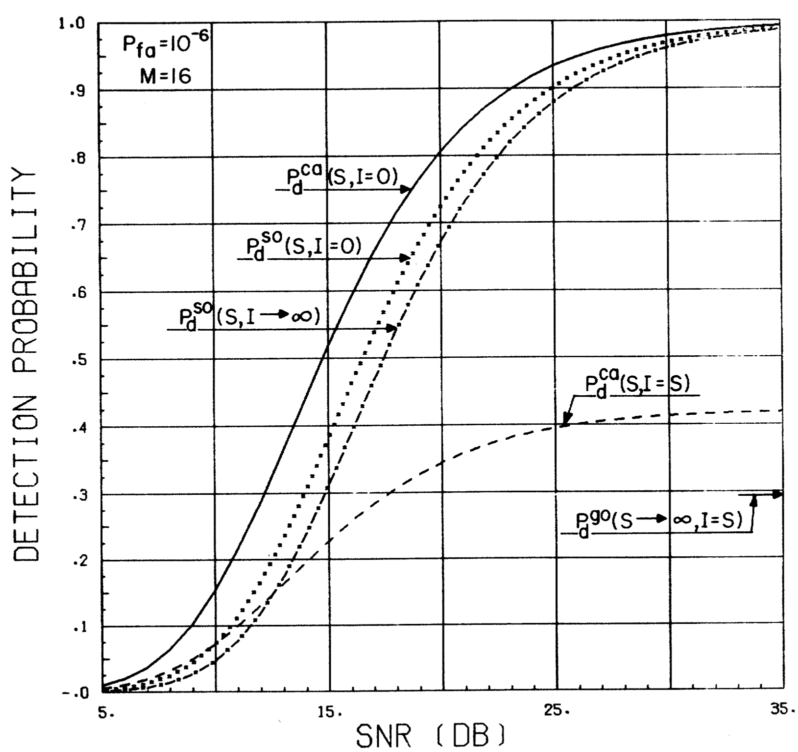

Fig. 8. Detection probability versus primary target SNR. P_d^{SO} $(S, I = 0)$: SO-CFAR without interfering target. P_d^{SO} $(S, I \rightarrow \infty)$: SO-CFAR with infinite SNR interfering target. P_d^{CA} $(S, I = S)$: CA-CFAR without interfering target. P_d^{CA} $(S, I = S)$: CA-CFAR with interfering target whose SNR is equal to primary's. P_d^{GO} $(S \rightarrow \infty, I = S)$: GO-CFAR when both targets have equal and infinite SNR ($P_{fa} = 10^{-6}$, $M = 16$).

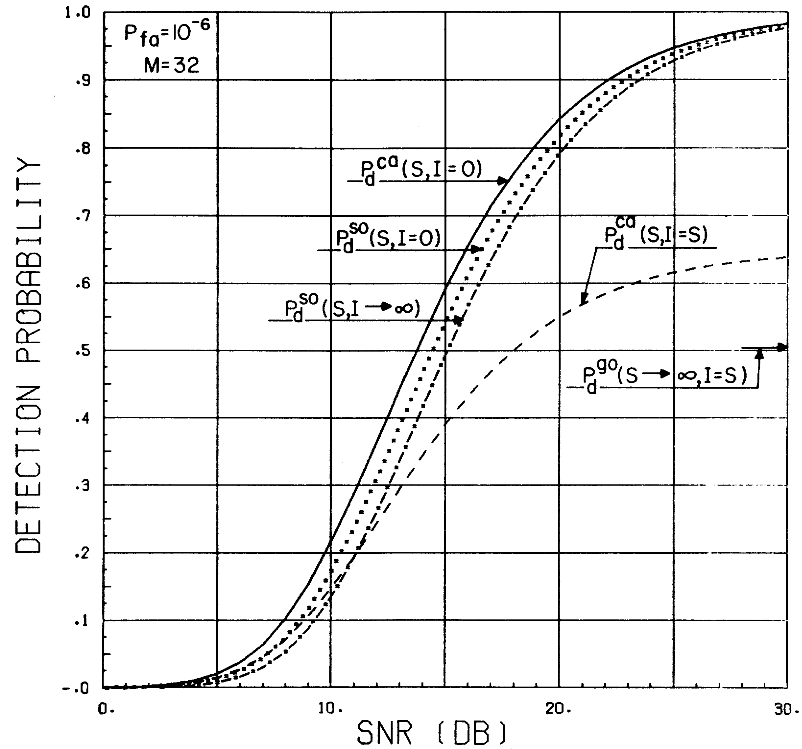

Fig. 9. Detection probability versus primary target SNR. P_d^{SO} $(S, I = 0)$: SO-CFAR without interfering target. P_d^{SO} $(S, I \to \infty)$: SO-CFAR with infinite SNR interfering target. P_d^{CA} $(S, I = S)$: CA-CFAR without interfering target. P_d^{CA} $(S, I = S)$: CA-CFAR with interfering target whose SNR is equal to primary's. P_d^{GO} $(S \to \infty, I = S)$: GO-CFAR when both targets have equal and infinite SNR ($P_{fa} = 10^{-6}$, $M = 32$).

P_d. This loss can be expressed in a closed form by substituting (17) [with $I = 0$ and (22) into (20)]

$$L_{SO}(I \to \infty) = 10 \log[I_{SO}(P_{fa}, M)/(P_d^{-2/M} - 1) - 1]/ \{[(P_d/P_{fa})^{1/M} - 1]/(1 - P_d^{1/M})\}. \quad (23)$$

The losses corresponding to the same values of P_{fa} and M as before are summarized in Table VI. Comparing it with Table V, we see that even in this severest case when the interfering target is of an infinite SNR, it merely produces a moderate additional sensitivity loss (relative to $\Delta L_{SO}(0)$ which has been shown to be quite large for small M). It is expected that for practical values of I, the difference $\Delta L_{SO}(I) - \Delta L_{SO}(0)$ would be much smaller. The cause for this additional loss is, obviously, the nonzero probability that the window output which contains the interfering target, will be selected for the adaptive threshold.

TABLE VI
SO-CFAR Additional Loss δL_{SO} $(I \to \infty)$, (dB), versus M and P_{fa}, With an Interfering Target of Infinite SNR ($P_d = 0.5$)

	M			
P_{fa}	4	8	16	32
10^{-4}	8.62	3.90	1.97	1.07
10^{-6}	13.2	5.84	2.71	1.35
10^{-8}	18.1	7.96	3.50	1.69

V. DISCUSSION

The tradeoffs to be compromised, concerning selection of the appropriate type of processor and an adequate choice of M, are manifold and highly dependent on the specific clutter and interference models assumed, in particular in a nonhomogeneous environment. Therefore, an optimal and general purpose CFAR detector can almost never be devised.

When M is increased, the CFAR loss (for all the three detector types considered in this paper) in a stationary noise background monotonically decreases to zero, together with an increased hardware complexity, and an inevitable violation of the inherent assumption that the noise samples are identically distributed over the reference window and properly represent the noise in the detection cell. Therefore, in a nonhomogeneous environment the CFAR penalty sometimes increases with M for large M; also, the likelihood that an interfering target or a "spiky" clutter return has entered the reference window is obviously larger for larger M. On the other hand, once the window has been captured by the interfering target, the primary target is less suppressed with larger M. As for the detector type, the SO-CFAR is almost not affected by the interfering target, while the suppression effect is serious in the CA-CFAR and even worse in the GO-CFAR

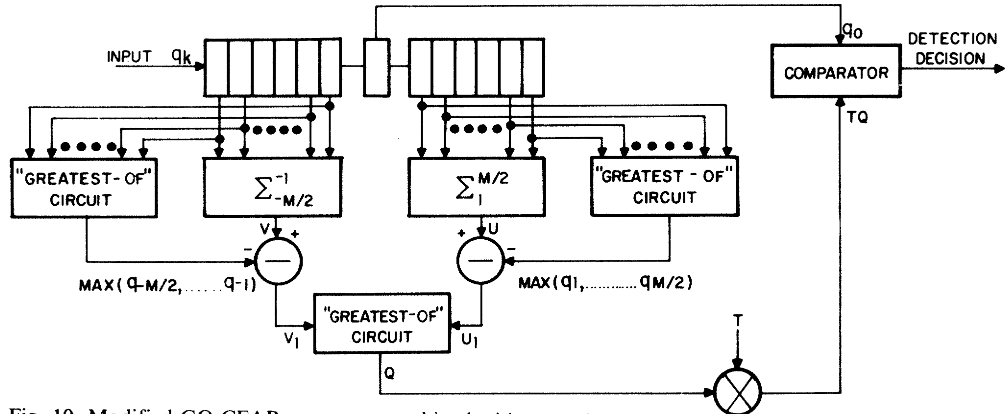

Fig. 10. Modified GO-CFAR processor combined with censoring circuit for one interfering target.

(which, however, is the best at clutter edges). Practically, when $M \leqslant 16$ detection of target pairs with the GO-CFAR is almost totally inhibited.

If, in some specific radar processor design, a high clutter rejection could be achieved (by some MTI or pulse-Doppler processing) such that the residue background level variations are relatively weak (say, a few decibels), it is suggested as in [14] that the SO-CFAR should be used for minimization of the capture effect, but with M large enough (corresponding to the required P_{fa} and minimum detectable signal) such that the sensitivity loss is tolerable. If this is not possible and clutter edges are expected to be too sharp, the GO-CFAR should be used along with some means of censoring large returns from the reference cells.

A censoring algorithm was proposed by Urkowitz and Perry [16], and a modification of it which is applicable to a distribution-free detector by Trunk et al. [13]. A secondary threshold (which is also adaptive) is generated, and each of the reference cells[3], outputs that are higher than it are discarded from the mean Q. This technique was shown [13] to be very effective. However, the following major addition in hardware is needed: a processor of M reference cells requires 3 M-tap delay lines, M coincidence-gates (analog multipliers), 2 comparators, 2 adders (op-amplifiers), and 2 analog multipliers.

A different algorithm which demands less hardware was presented and analyzed by Rickard and Dillard [12]. The tap outputs comprising the sum Q are ranked according to their magnitude, the K largest ranks are discarded from Q, and a new mean Q_k is formed from the remaining outputs. This detector effectively copes with k interfering targets. A combination of this censoring algorithm (for $k = 1$) with the GO-CFAR detector is shown in Fig. 10. The ranker in this case is a "GO $M/2$" circuit and is composed of $M/2 - 1$ analog comparators. Although the performance of this modified GO-CFAR processor has not been analyzed, we believe that it can function adequately in a complex nonhomogeneous environment, consisting of both clutter edges and closely separated targets, and that it can minimize either excessive false alarms or detection suppression effects.

APPENDIX A

THE PDF OF THE REFERENCE WINDOW CONTAINING INTERFERING TARGET

The output of the leading window V is written as a sum of two independent random variables

$$V = \sum_{i=1}^{M/2-1} q_i + q_{M/2} \triangleq X + Y. \tag{A1}$$

Y represents the output of the (arbitrary) cell containing the interfering target, and its pdf is $P_y(Y) = {}_1P_q(Y, S \rightarrow I, \sigma = 1)$. Obviously,

$$P_x(X) = X^{M/2-2} \exp(-X)/(M/2-2)!, \qquad X \geqslant 0. \tag{A2}$$

The pdf of V is obtained from the convolution integral

$$P_v(V) = \int_0^v P_x(X)\, P_y(V - x)\, dx. \tag{A3}$$

Direct evaluation of the integral, using

$$\int_0^Q x^N e^{-Ax} dx = (N!/A)\{1/A^n - \exp(-AQ) \cdot \sum_{K=0}^{N} [Q^{N-K}/(N-K)!\, A^K]\} \tag{A4}$$

leads to the result given in (11). Integration of (11) is also straightforward and thus (12) is obtained. When $I = 0$, the limiting form of (11) is found by applying L'Hôpital's rule, which results in the χ^2 distribution (9).

APPENDIX B

DETECTION PROBABILITY OF GO-CFAR FOR INFINITE I

When the SNR of the interfering target I is very large, the asymptotic forms of (11) and (12) are

$$\lim_{I \to \infty} P_v(V) = (1/I) \exp(-V/I) \tag{B1}$$

$$\lim_{I \to \infty} F_v(V) = 1 - \exp(-V/I). \tag{B2}$$

The following is equivalent to an upper bound for $P_d^{GO}(S, I)$ which is obtained by observing that P_d is less than the probability that q_0 exceeds only the threshold which is the greatest of the U window and the cell output which contains the interfering target [12].

Thus the pdf of the reference estimator is obtained by substituting (B1) and (B2) along with (9) and (10) into (7)

$$\lim_{I \to \infty} P_Q^{GO}(Q) = [Q^{M/2-1} \exp(-Q)/(M/2-1)!] \cdot [1 - \exp(-Q/I)] + (1/I) \exp(-Q/I) \cdot [1 - \exp(-Q) \sum_{k=0}^{M/2-1} (Q^K/K!)], \qquad Q \geqslant 0. \tag{B3}$$

Using (B3) and (4) in (3) gives

$$\lim_{I \to \infty} P_d^{GO}(S, I) = (1+S)/(1+S+I\,T_{GO}) + (1+S)^{M/2}[1/(1+S+T_{GO})^{M/2}] - \{I/[(1+S+T_{GO})I + 1 + S]\}^{M/2} - (1/I) \cdot \sum_{k=0}^{M/2-1} \{I(1+S)/[(1+S+T_{GO}) \cdot I + 1 + S]\}^{M/2-k}. \tag{B4}$$

Therefore, when the SNR of the primary target is also very large but the ratio I/S remains constant, the limit of (B3) is given by the first term, i.e.,

$$\lim_{\substack{I,\, S \to \infty \\ I,\, S \text{ constant}}} P_d^{GO}(S, I) = [1 + (I/S)T_{GO}(P_{fa}, M)]^{-1}. \tag{B5}$$

REFERENCES

[1] Finn, H.M., and Johnson, R.S. (1968)
Adaptive detection mode with threshold control as a function of spatially sampled clutter-level estimates.
RCA Review, Sept. 1968, *29*, 414-464.

[2] Nitzberg, R. (1970)
Application of invariant hypothesis testing techniques to signal processing.
Ph.D. dissertation, Syracuse University, NY, 1970.

[3] Scharf, L.L., and Lyte, D.W. (1971)
Signal detection in Gaussian noise of unknown level: An invariance application.
IEEE Transactions on Information Theory, July 1971, *IT-17*, 404-411.

[4] Steenson, B.O. (1968)
Detection performance of a mean-level threshold.
IEEE Transactions on Aerospace and Electronic Systems, July 1968, *AES-4*, 529-534.

[5] Mitchell, R.L., and Walker, J.F. (1971)
Recursive methods for computing detection probabilities.
IEEE Transactions on Aerospace and Electronic Systems, July 1971, *AES-7*, 671-676.

[6] Hansen, V.G. and Ward, H.R. (1972)
Detection performance of the cell-averaging LOG/CFAR receiver.
IEEE Transactions on Aerospace and Electronic Systems, Sept. 1972, *AES-8*, 648-652.

[7] Dillard, G.M. (1974)
Mean-level detection of nonfluctuating signals.
IEEE Transactions on Aerospace and Electronic Systems, Nov. 1974, *AES-10*, 795-799.

[8] Nitzberg, R. (1978)
Analysis of the arithmetic mean CFAR normalizer for fluctuating targets.
IEEE Transactions on Aerospace and Electronic Systems, Jan. 1978, *AES-14*, 44-47.

[9] Hansen, V.G. (1973)
Constant false alarm rate processing in search radars.
In *Proceedings of the IEE 1973 International Radar Conference*, London, 1973, 325-332.

[10] Moore, J.D., and Lawrence, N.B. (1980)
Comparison of two CFAR methods used with square law detection of Swerling I targets.
In *Proceedings of the IEEE International Radar Conference*, Arlington, VA, Apr. 1980, 403-409.

[11] Hansen, V.G., and Sawyers, J.H. (1980)
Detectability loss due to greatest of selection in a cell-averaging CFAR.
IEEE Transactions on Aerospace and Electronic Systems, Jan. 1980, *AES-16*, 115-118.

[12] Rickard, J.T., and Dillard, G.M. (1977)
Adaptive detection algorithms for multiple target situations.
IEEE Transactions on Aerospace and Electronic Systems, July 1977, *AES-13*, 338-343.

[13] Trunk, G.V., Cantrell, B.H., and Queen, F.D. (1974)
Modified generalized sign test processor for 2-D radar.
IEEE Transactions on Aerospace and Electronic Systems, Sept. 1974, *AES-10*, 574-582.

[14] Trunk, G.V. (1978)
Range resolution of targets using automatic detectors.
IEEE Transactions on Aerospace and Electronic Systems, Sept. 1978, *AES-14*, 750-755.

[15] Papoulis, A. (1965)
Probability, Random Variables, and Stochastic Processes.
New York: McGraw-Hill, 1965.

[16] Urkowitz, H., and Perry, R.P. (1973)
A CFAR techinique insensitive to nearby targets.
RCA, Systems Technology Memo STM-11011, May 18, 1973.

Moshe Weiss was born in Gallaty, Rumania, on August 8, 1947. Following service as a Commanding Officer in the IDF from 1965 to 1970, he received the B.Sc. and M.Sc degrees in electrical engineering from Technion—Israel Institute of Technology, Haifa, in 1974 and 1979, respectively.

Since 1974 he has worked for RAFAEL—Armament Development Authority, Haifa, Israel, on various projects of radar and communication systems design and analysis and is presently a group leader.